# Real-Time Tracking of Singlet Exciton Diffusion in Organic Semiconductors

Oleg V. Kozlov, Foppe de Haan, Ross A. Kerner, Barry P. Rand, David Cheyns, and Maxim S. Pshenichnikov

Phys. Rev. Lett. **116**, 057402 — Published 4 February 2016

DOI: 10.1103/PhysRevLett.116.057402

**Real-time tracking of singlet exciton diffusion in organic semiconductors**

Oleg V. Kozlov[1], Foppe de Haan[1], Ross A. Kerner[2], Barry P. Rand[2], David Cheyns[3], Maxim S. Pshenichnikov[1*]

[1]Zernike Institute for Advanced Materials, University of Groningen, 9747AG Groningen, The Netherlands

[2]Department of Electrical Engineering and Andlinger Center for Energy and the Environment, Princeton University, Princeton, NJ, 08544 USA

[3]*imec*, B3001 Leuven, Belgium.

Exciton diffusion in organic materials provides the operational basis for functioning of such devices as organic solar cells and light-emitting diodes. Here we track the exciton diffusion process in organic semiconductors in real time with a novel technique based on femtosecond photoinduced absorption spectroscopy. Using vacuum-deposited $C_{70}$ layers as a model system, we demonstrate an extremely high diffusion coefficient of $D \approx 3.5 \cdot 10^{-3}$ cm$^2$/s that originates from surprisingly low energetic disorder of <5 meV. The experimental results are well-described by the analytical model and supported by extensive Monte-Carlo simulations. The proposed noninvasive time-of-flight technique is deemed as a powerful tool for further development of organic opto-electronic components, such as simple layered solar cells, light-emitting diodes, and electrically pumped lasers.

Electronic devices based on organic semiconductors have attracted much interest over the last decades as an alternative to conventional inorganic electronics [1], largely due to their chemically-tunable optical properties [2]. Organic electronic devices, such as organic solar cells (OSCs) and light-emitting diodes (OLEDs) rely on the ability of Frenkel excitons either to dissociate at the interface between *p*- and *n*-type materials to produce separated charges or to recombine within the recombination layer to produce photon emission [3,4]. The efficiency of the aforementioned devices directly depends on the exciton diffusion within the active layer. In general, there are three parameters characterizing the exciton diffusion in the semiconducting layer: the exciton lifetime $T_1$, the diffusion coefficient $D$ and the diffusion length $L_d$, interconnected via the relation $L_d \sim \sqrt{DT_1}$ [4]. The singlet exciton lifetime $T_1$is relatively easy to measure by e.g. the time-resolved fluorescence [5], while obtaining either $D$ or $L_d$ is much more challenging because of the tens-nm length scale over which the Frenkel excitons diffuse.

Various techniques to measure $L_d$ and/or $D$ have been proposed and utilized to date [3,4,6-10] which roughly fall into the following two categories. Spectroscopic techniques rely on photoluminescence quenching [9,11,12], or on a highly non-equilibrium process of exciton-exciton annihilation [13]. Charge carrier techniques observe time-averaged charge yield after exciton dissociation and as a consequence necessitate either the modeling of the external quantum efficiency of the operating device [14,15] or microwave/photoconductivity measurements [16,17]. Spectroscopic methods provide high temporal resolution; however, they require strongly photoluminescent (PL) materials [6], while the charge yield does not necessary correlate with the efficiency of PL quenching [18]. In turn, charge carrier techniques do not possess time resolution and therefore miss dynamical aspects of exciton dynamics [4].

The advantages of both approaches can be combined in a new technique that provides a direct handle on the exciton diffusion coefficient. Similarly to the spectroscopic techniques, the material of interest (absorber) with known thickness is covered by an exciton quencher, the hole (or electron) accepting layer (Fig. 1). After spectrally-selective photoexcitation of the absorber by the ultrashort visible pulse, the photogenerated excitons diffuse to the interface with the quencher where they dissociate into pairs of charges. The concentration of charges (holes) in the quencher is measured - similarly to the charge carrier techniques - but now in the time-resolved fashion via photoinduced polaron absorption (PIA) [22] (Fig. 1(b)). The resulting transient alone yields the exciton diffusion coefficient; therefore, only a single sample of well-defined thickness is required.

Here we apply the new method for real-time tracking of singlet exciton diffusion to vacuum-deposited layers of the well-known OSC acceptor, $C_{70}$ fullerene. We demonstrate efficient singlet exciton harvesting from $C_{70}$ layers up to 70 nm in thickness. The exciton diffusion process is temperature-independent down to 77 K, which implies extremely low energetic disorder of <5 meV. The experimental findings are excellently described by a simple analytical model and also supported by extensive Monte-Carlo simulations.

In our experiments, vacuum-deposited $C_{70}$ layers of different thicknesses from 6 nm to 196 nm (absorber) are sandwiched between 10 nm thick layers of tris[4-(5-phenylthiophen-2-yl)phenyl]amine (TPTPA) which acts as a quencher and hole acceptor. All the TPTPA/C70 and C70/TPTPA interfaces are measured to be abrupt in the limit of molecular roughness [11, 24].

PIA measurements were performed in a standard pump-probe arrangement at a visible-pump, IR-probe setup based on a Spectra-Physics Hurricane system (~120 fs, 800 nm, 1 KHz repetition rate) and two optical parametrical amplifiers (Light Conversion TOPAS). The

polarization of the probe pulse was set at the magic angle of 54.7° with respect to the polarization of excitation pulse to observe the population signal only [25]. After the sample, the IR signal was detected by nitrogen-cooled InSb detectors, transmission change $\Delta T$ of the sample with and without the excitation pulse was calculated and normalized on the sample transmission $T$ as $\Delta T/T$. To minimize the biexciton recombination and ensure linearity of the response at all delay times the energy density of the excitation pulse was decreased to ~1.3 μJ/cm$^2$, which corresponds to the average photon density of $3 \cdot 10^{-4}$ nm$^{-3}$. For a more detailed description of the experiment, see Supplemental Material [23].

Figure 2(a) shows absorption spectra of TPTPA and $C_{70}$ layers. $C_{70}$ exhibits strong absorption below 700 nm while the TPTPA film absorption peaks at 400 nm so that the excitation wavelength of 530 nm was chosen to selectively excite $C_{70}$; lower-wavelength excitation yielded similar results [23]. To evaluate the position of the polaron absorption peak in the TPTPA molecule, the dependence of the response on the probe wavelength was measured at different delay times (Fig. 2(b)). The polaron spectra show a broad peak in the near-IR region centered around 1.5 μm, consistent with previous data on similar star-shaped molecules [26]. The position of the absorption peak remains unchanged with the pump-probe delay which indicates an absence of spectral diffusion due to, for instance, polaron relaxation. Therefore, the hole polarons are monitored at the constant probe wavelength of 1.55 μm. At this wavelength, maximal IR response of pure $C_{70}$ films (due to excited state absorption of singlet and/or triplet excitons in $C_{70}$ [27,28]) is by a factor of ~6 weaker than the resonant TPTPA response, and is readily accounted for [23].

The time-of-flight dynamics of exciton harvesting from $C_{70}$ layers of different thicknesses from 6 nm to 192 nm, are shown in Fig. 3. The transients represent the accumulated

number of generated TPTPA holes via $C_{70}$ exciton dissociation (Fig.1(b)) and therefore their amplitudes are proportional to the amount of split excitons (i.e. those which have made it to the interfaces). All signals are normalized by the number of the photons absorbed so that harvesting efficiencies in different samples can be compared directly. At short times (<1 ps), the signal rises due to interfacial excitons (i.e. excitons formed at the donor/acceptor interface) splitting into charges via the hole-transfer process [19]. This development is the most apparent in samples with thin $C_{70}$ layers where the share of interfacial excitons is statistically higher. At longer times, the signals increase gradually at a much slower timescale (up to ns) that is strongly dependent on the $C_{70}$ thickness. This time region is attributed to diffusion-delayed splitting of excitons generated within the $C_{70}$ layer.

The total number of diffusion-delayed excitons split at the interface by time *t* (i.e. the number of accumulated holes) is readily obtained by solving the 1D exciton diffusion equation with the zero Dirichlet boundary conditions [4,29] (see [23] for details):

$$H_b(t) = \frac{DT_1}{L}\sum_{m=1}^{\infty}[P(0) - (-1)^m P(L)]B_m\left(\frac{\pi m}{L}\right)\frac{1-e^{-t\left(\frac{1}{T_1}+\left(\frac{\pi m}{L}\right)^2 D\right)}}{1+\left(\frac{\pi m}{L}\right)^2 DT_1} \quad (1)$$

where *D* is the diffusion coefficient, *L* is the thickness of the $C_{70}$ layer, *P(0)* and *P(L)* are the (relative) intensity of the probe at the two interfaces, $T_1$ is $C_{70}$ exciton effective lifetime of 500 ps obtained from time-resolved photoluminescence (PL) measurements [5,30] and

$$B_m = \frac{2}{L}\int_0^L I(z)\sin(\omega_m z)dz \quad (2)$$

where *I(z)* is the initial distribution of the exciton density along the *z*-axis. Because of optical interference in the thin layered samples [31-34], *P(z)* and *I(z)* were calculated separately using a transfer-matrix method [35].

In Eq.(1), the only unknown parameter is the diffusion coefficient $D$, which can be directly obtained by fitting each individual transient (Fig. 3, solid lines). The diffusion coefficients are grouped around $D \approx 3.5 \cdot 10^{-3}$ cm$^2$/s (Fig. 4(a)) so that a single sample could be used to obtain the diffusion coefficient. The obtained diffusion coefficient is a factor of 15 higher than for the prototypical solution-processed organic solar cell acceptor material, $PC_{71}BM$ [36]. For the thin samples (<12 nm), the diffusion coefficients are somewhat higher due to a relatively high share of near-interfacial excitons (~20% for 12 nm sample) which undergo ballistic rather than diffusional trajectories and therefore are not accounted for by the diffusion equation.

An alternative way to obtain the diffusional coefficient is to examine the efficiency $\eta$ of exciton harvesting (i.e. the maximal amplitudes of the transients) as a function of $C_{70}$ layer thickness (Fig. 4(b)) and fit it with the well-known relation [29]:

$$\eta(L) = \frac{2\sqrt{DT_1} * tanh(\frac{L}{2\sqrt{DT_1}})}{L} \quad (3)$$

The fit resulted in $D \approx 3 \cdot 10^{-3}$ cm$^2$/s which is in excellent agreement with the single-transient approach (Fig.4(a)). Exciton harvesting efficiency decreases with increasing layer thickness because of the finite $C_{70}$ singlet exciton effective lifetime of ~500 ps , mainly due to intersystem crossing to the triplet state [5,28]). The excitons are efficiently harvested from the 70 nm layer if we define it as a thickness at which the harvesting efficiency falls to the $e^{-1}$ level for direct comparison with the light penetration depth of ~80 nm at 530 nm in $C_{70}$ films [23]. Previously, $L_d$ ranging from 7 to 40 nm has been reported for the $C_{60}$ fullerene [31,37] but were recently attributed to triplets [16]; the results for $C_{70}$ are also widely spread from 7 to 29 nm [38,39]. We note that wide spread of these values most probably originates from indirect measurements relying on modeling of the external quantum efficiency; in contrast, our measurements directly demonstrate the long exciton harvesting distances in $C_{70}$.

As $C_{70}$ produces weak but nonetheless detectable PL, our results can be benchmarked against conventional time-resolved PL quenching method [4,6,29,40,41]. It turns out that a single-transient approach (similar to the one depicted Figs.3 and 4a) does not produce stable results especially for thick samples [23]. Nonetheless, from the combined dependence of quenching efficiency on the $C_{70}$ layer thickness (i.e. from essentially multisampling approach as opposed to single-sample PIA), we obtained the diffusion coefficient of $D \approx 4 \cdot 10^{-3}$ cm$^2$/s, which is fairly close to the values cited above.

The analytical model presented by Eq.1 makes several implicit assumptions (such as a flat energy landscape, localized excitons, negligible exciton annihilation) that in general are not granted. To verify their significance, Monte-Carlo simulations were performed to model exciton motion in a 3D random walk within a cubic disordered grid [23]. It appears that the excitons are delocalized within approximately four $C_{70}$ molecules, which is in good agreement with previous findings on delocalization effects in fullerenes [42], and the share of annihilated excitons is relatively low (<10% even for the thickest samples). The energetic Gaussian disorder [43] resulting from simulations is ~5 meV, i.e. negligibly low compared to $kT$ ~26 meV at 297 K. This implies that the diffusion process should not change substantially down to nitrogen temperatures of 77 K which was confirmed to be the case (Fig. 4(a), inset). The low disorder (and, as a result, high diffusion rate) most probably sources from the symmetry of the $C_{70}$ molecule and vacuum deposition process used to prepare the films.

In summary, we have demonstrated efficient exciton harvesting from vacuum-deposited $C_{70}$ layers up to 70 nm thick with the unique time-of-flight spectroscopic approach that allows obtaining the diffusion coefficient and exciton harvesting distances from a single sample. The experimental data are perfectly described by a simple analytical model, allowing us to obtain the

diffusion rate of $D \approx 3.5 \cdot 10^{-3}$ $c\text{m}^2/\text{s}$ from a single sample. We foresee the proposed noninvasive time-of-flight technique as a powerful tool for further development of organic opto-electronic components, such as simple layered solar cells [44], thin-film light-emitting transistors, and electrically pumped lasers.

O.V.K. acknowledges support by "Aurora – Towards Modern and Innovative Higher Education" Programme. R.A.K. and B.P.R. acknowledge support by the U.S. Department of Energy, Office of Basic Energy Sciences, Division of Materials Sciences and Engineering under Award #DE-SC0012458.

* m.s.pchenitchnikov@rug.nl

**Figures**

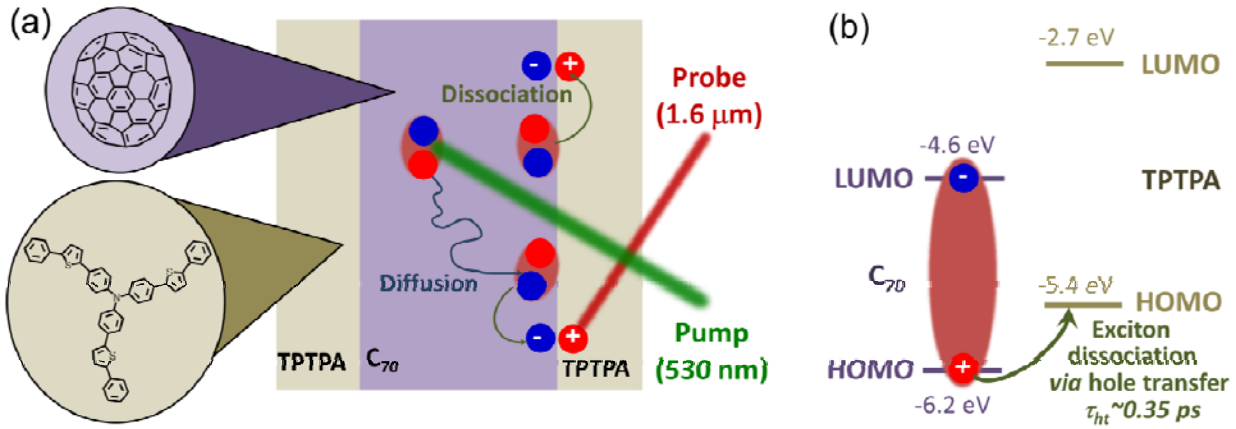


FIG. 1 (color online). Experimental concept. (a) Schematic of the time-of-flight experiment, and molecular structures of TPTPA (donor) and $C_{70}$ (acceptor). (b) Energetics of $C_{70}$ exciton (shown as the brown oval) dissociation via hole transfer process [19]. Energy levels of $C_{70}$ and TPTPA are taken from Refs. [20,21].

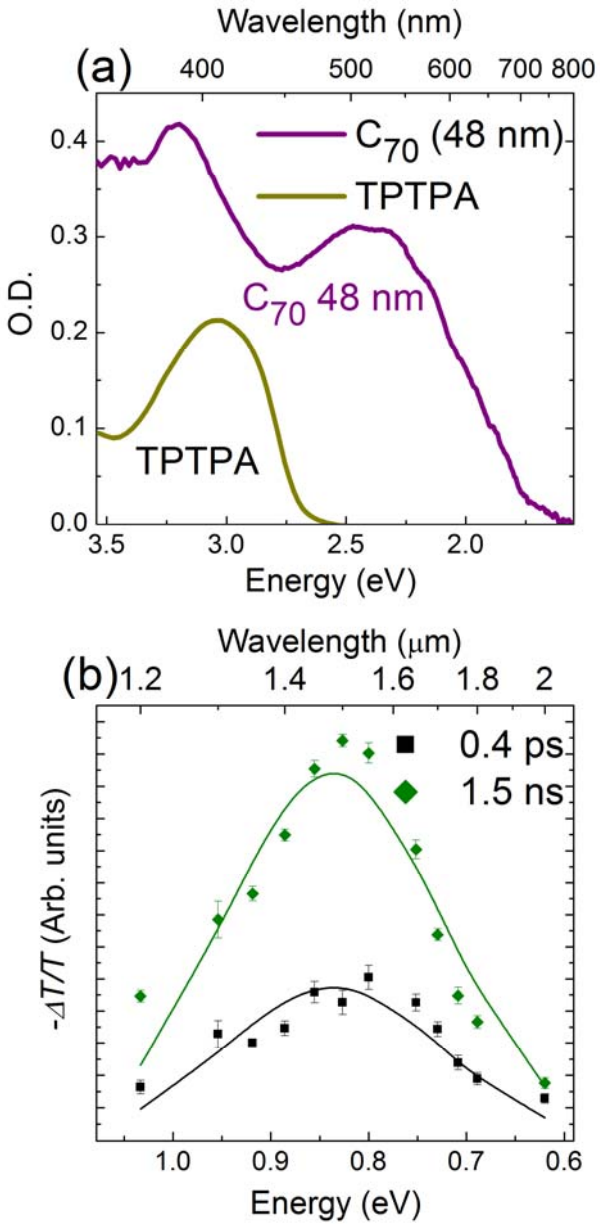


FIG. 2 (color online). (a) Absorption spectra of 48 nm $C_{70}$ (purple) and 12 nm TPTPA (yellow) samples. (b) Polaron absorption spectra for the 6 nm sample at 0.4 ps (black squares) and 1.5 ns (green diamonds) delays; for other polaron spectra, see Figure S4 in Ref.[23]. Solid lines are fits with Gaussian functions. The excitation wavelength is 530 nm.

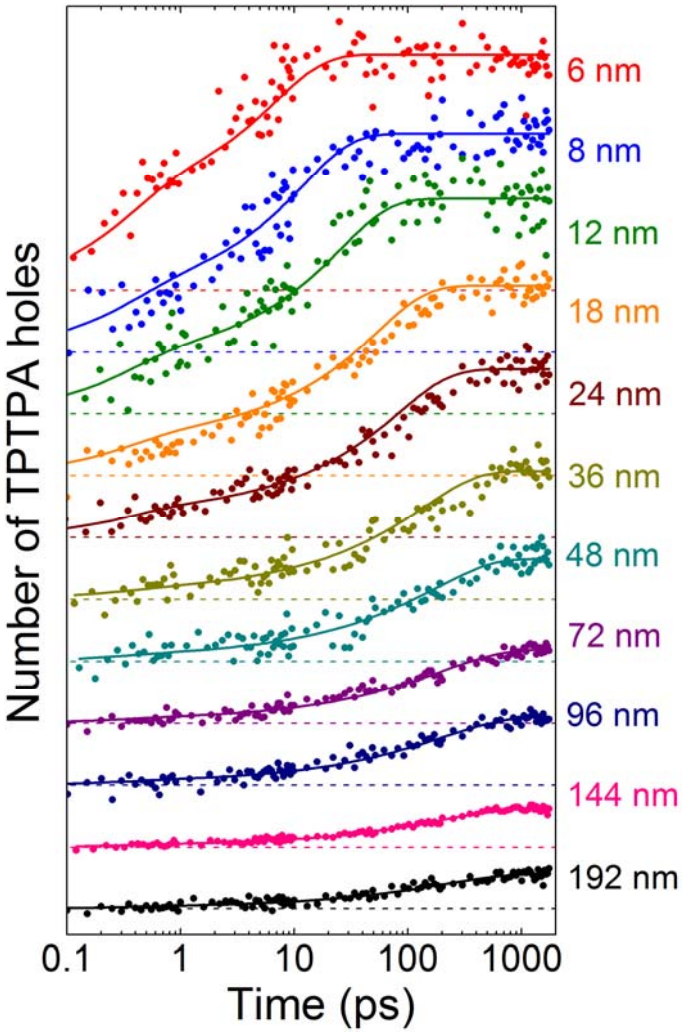


FIG. 3 (color online). Measured (dots) and fitted with analytical model (solid lines) transients for different samples. Each transient is offset by $\Delta T/T=2\cdot10^{-4}$ to the corresponding dashed line; the thickness of each $C_{70}$ layer is indicated to the right. All transients are normalized by the number of absorbed photons and corrected for the $C_{70}$ contribution (see [23] for details).

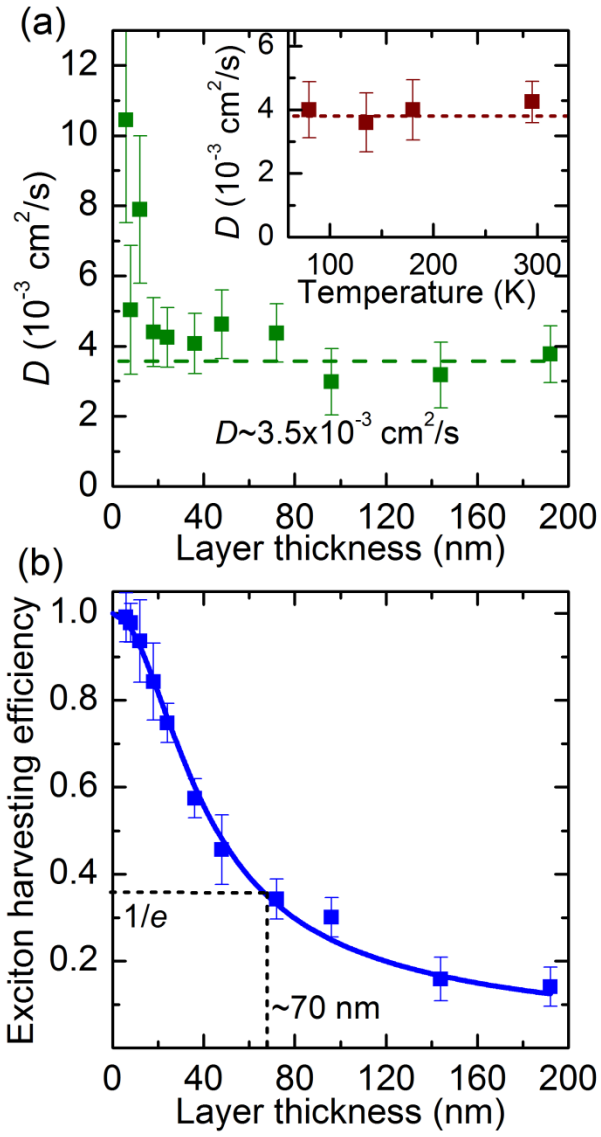


FIG. 4 (color online). (a) Exciton diffusion coefficients obtained from independent fits of each transient. The inset shows the temperature dependence of the diffusion coefficient for the 24 nm thick sample. (b) Exciton harvesting efficiency *vs.* $C_{70}$ layer thickness. The experimental values are shown by symbols while the solid line is obtained from a fit to Eq.3. The data are corrected for the exciton annihilation. For the thinnest sample (6 nm), a 100% exciton harvesting efficiency is assumed.

**References**


[1] T. W. Kelley *et al.*, Chem.Mat. **16**, 4413 (2004).

[2] R. R. Lunt and V. Bulovic, Appl. Phys. Lett. **98**, 113305 (2011).

[3] A. Kohler and H. Bassler, *Electronic Processes in Organic Semiconductors: An Introduction* (Wiley-VCH Verlag GmbH & Co. KGaA, Weinheim, Germany, 2015).

[4] O. V. Mikhnenko, P. W. M. Blom, and T.-Q. Nguyen, En. Env. Science **8**, 1867 (2015).

[5] S. Reindl, A. Penzkofer, and H. Gratz, J. Photochem. Photobiol. A: Chem. **115**, 89 (1998).

[6] S. M. Menke and R. J. Holmes, En.Env. Science **7**, 499 (2014).

[7] O. V. Mikhnenko *et al.*, Phys. Rev. Lett. **108**, 137401 (2012).

[8] S. Westenhoff, I. A. Howard, and R. H. Friend, Phys. Rev. Lett. **101**, 016102 (2008).

[9] A. Haugeneder *et al.*, Phys. Rev. B **59**, 15346 (1999).

[10] D. E. Markov *et al.*, Phys. Rev. B **72**, 045216 (2005).

[11] D. E. Markov *et al.*, J. Phys. Chem. A **109**, 5266 (2005).

[12] O. V. Mikhnenko *et al.*, Adv. Mat. **26**, 1912 (2014).

[13] A. J. Lewis *et al.*, Org. Elect. **7**, 452 (2006).

[14] Y. Terao, H. Sasabe, and C. Adachi, Appl. Phys. Lett. **90**, 103515 (2007).

[15] S. Banerjee *et al.*, Appl. Phys. Lett. **94**, 223303 (2009).

[16] M. C. Fravventura *et al.*, J. Phys. Chem. Lett. **3**, 2367 (2012).

[17] H. Najafov *et al.*, Nat Mater **9**, 938 (2010).

[18] S. D. Dimitrov and J. R. Durrant, Chem. Mat. **26**, 616 (2014).

[19] A. A. Bakulin *et al.*, Adv. Funct. Mat. **20**, 1653 (2010).

[20] D. Kekuda *et al.*, Solar En. Mat. and Solar Cells **94**, 1767 (2010).

[21] P. D. Reusswig *et al.*, Appl. Phys. Lett. **101**, 113304 (2012).

[22] X. Wei *et al.*, Phys. Rev. B **53**, 2187 (1996).

[23] See Supplemental Material at [URL will be inserted by publisher] for detailed description of experiment and models as well as additional experimental data.

[24] A. Neuhold *et al.*, Org. El. **14**, 479 (2013).

[25] R. G. Gordon, J. Chem. Phys. **45**, 1643 (1966).

[26] O. V. Kozlov *et al.*, Adv. En. Mat. **5**, 1401657 (2015).

[27] R. V. Bensasson *et al.*, Chem. Phys. Lett. **206**, 197 (1993).

[28] J. W. Arbogast and C. S. Foote, J. Am. Chem. Soc. **113**, 8886 (1991).

[29] O. V. Mikhnenko *et al.*, J. Phys. Chem. B **112**, 11601 (2008)

[30] A. Watanabe *et al.*, J. Phys. Chem. **100**, 10518 (1996).

[31] P. Peumans, A. Yakimov, and S. R. Forrest, J. Appl. Phys. **93**, 3693 (2003).

[32] D. Qin *et al.*, Phys. Stat. Solidi (a) **208**, 1967 (2011).

[33] F. Monestier *et al.*, Appl. Opt. **47**, C251 (2008).

[34] T. Stübinger and W. Brütting, J. Appl. Phys. **90**, 3632 (2001).

[35] L. A. A. Pettersson, L. S. Roman, and O. Inganäs, J. Appl. Phys. **86**, 487 (1999).

[36] G. J. Hedley *et al.*, Nat. Comm. **4**, 2867 (2013).

[37] O. Runquing, R. A. Gerhardt, and R. J. Samuels, J.Pol.Scien.: Part B: Polymer Phys. **42**, 98 (2004).

[38] B. Verreet *et al.*, Appl.Phys. Lett. **102**, 043301 (2013).

[39] T.-M. Kim *et al.*, ACS Appl. Mat. & Int. **6**, 4286 (2014).

[40] J. D. A. Lin *et al.*, Mat. Horiz. **1**, 280 (2014).

[41] E. M. Y. Lee and W. A. Tisdale, J. Phys. Chem. C **119**, 9005 (2015).

[42] B. Bernardo *et al.*, Nat Comm. **5**, 3245 (2014).

[43] K. Feron *et al.*, Int. J. Mol. Scien. **13**, 17019 (2012).

[44] D. Cheyns *et al.*, Appl. Phys. Lett. **104**, 093302 (2014).